Received: 27 August 2019 | Revised: 17 October 2019 | Accepted: 5 November 2019

DOI: 10.1111/ffe.13163

ORIGINAL CONTRIBUTION

WILEY FFEMS Fatigue & Fracture of Engineering Materials & Structures

Fatigue strength of fillet-welded joints at subzero temperatures

Moritz Braun | **Robert Scheffer** | **Wolfgang Fricke** | **Sören Ehlers**

Institute for Ship Structural Design and Analysis, Hamburg University of Technology, Hamburg, Germany

Correspondence
M. Braun, Hamburg University of Technology, Institute of Ship Structural Design and Analysis (M-10), Am Schwarzenberg Campus 4(C), D-21073 Hamburg, Germany.
Email: moritz.br@tuhh.de

Abstract

Ships and offshore structures may be operated in areas with seasonal freezing temperatures and extreme environmental conditions. While current standards state that attention should be given to the validity of fatigue design curves at subzero temperatures, studies on fatigue strength of structural steel at subzero temperatures are scarce. This study addresses the issue by analysing the fatigue strength of welded steel joints under subzero temperatures. Although critical weld details in large welded structures are mostly fillet-welded joints, most published data are based on fatigue crack growth rate specimens cut out of butt-welded joints. This study analyses fillet-welded specimens at −20°C and −50°C against controls at room temperature. Significantly higher fatigue strength was measured in comparison to estimates based on international standards and data from design codes even at temperatures far below the allowed service temperature based on fracture toughness results.

KEYWORDS

ductile-brittle transition, fatigue testing, high-strength steel, low temperatures, temperature dependence of fatigue curves, weldment fatigue

1 | INTRODUCTION

Due to the large unexploited oil and gas reservoirs in Arctic regions, there has been a significant increase in ship traffic in Arctic regions; oil rigs and wind turbines have also been increasingly set up in areas with seasonal freezing temperatures. These structures, and their materials, must be designed to meet these environmental conditions. Although it is known that lower temperatures change the material properties of steel and their welded joints, the resulting effects are poorly understood so far; this is especially true for fatigue behaviour at subzero temperatures.[1]

While detrimental effects caused by high temperatures are well covered in literature and are addressed in international standards, few publications exist on the fatigue properties of welded steel joints for subzero temperatures.[2-10] Moreover, most of those studies focus on fatigue crack growth (FCG) rate testing for cryogenic applications. Data for structural steels subjected to temperatures relevant for Arctic conditions are especially scarce and—except for Bridges et al[3] and Li et al,[8] who tested longitudinal stiffeners and cruciform joints, respectively—all mentioned studies are based on tests with butt-welded joints.

Although Bridges et al[3] found an increase of fatigue strength of welded specimens at subzero temperatures,

the Lloyd's Register FDA ICE Fatigue Induced by Ice Loading procedure[11] did not change the fatigue design curves. Instead, it was explicitly stated that the design curves for room temperature (RT) shall be applied for fatigue assessment. The corresponding International Organization for Standardization standard ISO19906[12] states that "attention should be given to the validity of S-N curves with respect to low temperature application" for Arctic offshore structures; however, no guidance is given on how to verify the validity of S-N curves. Current standards focus almost exclusively on fracture toughness requirements to avoid brittle fracture.[13] Avoidance of brittle fracture shall be achieved by proving sufficient fracture toughness at temperatures as low as 30°C below the Lowest Anticipated Service Temperature (LAST).[14] For some Arctic locations, LAST can approach −40°C or lower; this results in hard to meet toughness requirements.[13] High-strength, thermomechanically rolled, fine-grained structural steel is necessary to meet those requirements. Current ship standards are limited to S460 structural steel, however, and maritime structures are often made of normal-strength or mild-strength steel since fatigue strength of welded joints shows only minor or no influence of the base material strength.[15] By analysing large data sets of fracture toughness tests, Walters et al[16] showed that mild strength steel often fulfils the requirements for much lower temperatures than required. Fracture toughness, however, is only one parameter that has to be taken into account for subzero temperature applications (see Hauge et al[13] for an extensive summary on relevant material properties for Arctic structures; in order to develop standards for the design of fixed Arctic offshore structures, they identified fatigue strength as one of the major parameters influencing design of such structures[13]).

Although extensive subzero temperature material and fatigue tests date back to the beginning of space exploration and the storage and transport of liquefied gases,[17] it only recently regained attention from researchers.[18] Due to increased Artic transport and interest in Arctic oil and gas exploration, fatigue strength of structural materials at subzero temperatures[3,19,20] is now a critical area of study. Design standards currently assume that low temperatures have no detrimental effect on the fatigue properties of steels at typical operating temperatures.[13] This assumption is based on fatigue crack growth (FCG) rate testing of different base material steel types at temperatures down to cryogenic temperatures.[21-29] This assumption holds for materials that feature face-centred cubic (fcc) crystal structures. Structural steels which belong to the class of ferritic materials having a body-centred cubic (bcc) crystal structure, however, suffer from reduced toughness below the ductile-to-brittle transition temperature (DBTT). At low temperatures (sometimes within the range of typical operating temperatures), the mechanism of stable crack growth behaviour changes from plastic blunting and tearing to cleavage-controlled brittle fracture. This transition is usually measured by fracture toughness or Charpy notch impact tests. While normal-strength steels usually show a gradual change in the governing fracture process, high strength steels have a narrow range of temperature for this transition (see Wallin[30]). Structural design requires that the DBTT remains below the anticipated service temperatures, with a mandatory safety margin. An increase in FCG rate was found simultaneously to the decrease in fracture toughness for bcc materials in tests at DBTT-range temperatures (described by Alvaro et al[18] as the fatigue ductile-brittle transition [FDBT], with corresponding fatigue transition temperature [FTT]). By performing FCG rate tests over a wide range of temperatures and scanning electron fracture surface investigations, Alvaro et al[31,32] and Fang et al[33] relate this behaviour to a change in striation process when ductile crack growth is superimposed by cleavage bursts, which are triggered by embrittlement of the material. For temperatures below RT but above the FTT, however, the FCG rate is significantly decreased; this extends the structure lifetime.[28,29,31-33] The relation between the FTT and DBTT is better understood for different structural steel base materials due to recent effort by the aforementioned research groups; however, the effect of temperature on fatigue properties of welded structures is scarcely investigated. Fracture toughness tests show that the DBTT is usually higher in the heat-affected-zone (HAZ) of welded structures than in the surrounding base material,[34] which is the reason that such tests have to be performed with the notch on the fusion line between the weld metal and the HAZ. Its implication on the fatigue properties of welded structures is, however, nonexistent due to the lack of comprehensive studies regarding the change of static and dynamic properties of welded joints at subzero temperatures.[1]

In the present study, welded normal and high strength steel joints are tested to analyse the fatigue strength under subzero temperatures. The aim of the paper is to present the change in fatigue strength and to assess the effect on fatigue assessment procedures for structures experiencing low service temperatures. For this purpose, two cruciform joint weld details with the two typical failures initiation sites at weld toes and weld roots are tested at RT, −20°C, and −50°C.

2 | TEST SETUP AND SPECIMENS

In order to assess the temperature effect on typical weld details, cruciform joints with nonpenetrating fillet welds

and two-sided transverse stiffeners—leading to weld root and weld toe failure, respectively—are chosen; these are presented in Figure 1 as polished and etched macrographs. Two-sided transverse stiffeners with weld toe failure are a typical structural detail in large welded structures containing stiffeners, while nonpenetrating cruciform joints with weld root failure are among the most critical weld details (since cracks are only visually discoverable once they have reached a significant size and have grown through the weld metal). The throat thickness of load-carrying fillet welds is usually chosen to prevent weld root failure; however, this study uses a throat thickness small enough to yield weld root failure in order to analyse the effect of low temperatures on weld root failure. To rule out material-based uncertainties of the welded joints, two series of each weld detail are tested made from different steel types; each series consists of about 10 specimens. The first is a S235 J2 + N normalized steel that is often used in ship structures and the second a S500G1 + M thermomechanically rolled, fine-grained structural steel. The chemical composition is listed in Table 1 and the measured mechanical properties in Table 2.

The Charpy V-notch test results confirm that the S500 structural steel has a high toughness, even at temperatures as low as −40°C. Although the S235J2 + N normal structural steel in this study also shows high toughness results for the base material, it is not usually used for structures exposed to Arctic conditions. As can be seen from Walters et al's[16] statistical evaluation of around 7000 data sets of S355 and S690 samples, 55% of delivered S355 structural steel plates and 72% of delivered S690 structural steel plates fulfil the toughness requirements for a design temperature of −55°C.

TABLE 2 Mechanical properties of steels used

	σ_{YS}, MPa	σ_{UTS}, MPa	e_f, %	CVN, J
S235J2 + N	356	445	38	>200 at −20°C
S500G1 + M	595	651	23	>120 at −40°C

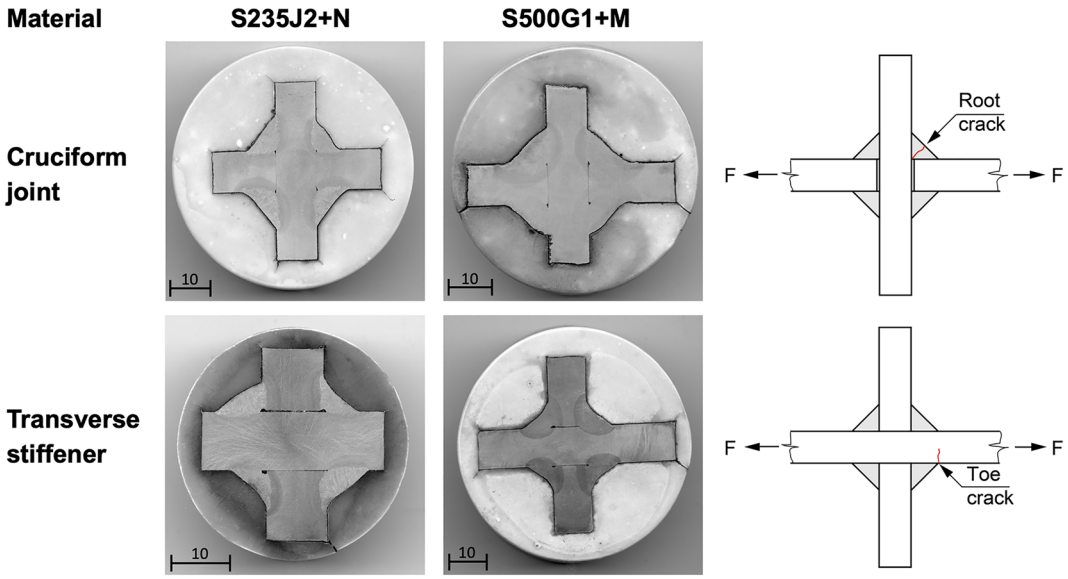

FIGURE 1 Polished and etched macrographs of cruciform joint and transverse stiffener fatigue test specimens and sketches indicating crack locations (scale in millimetres) [Colour figure can be viewed at wileyonlinelibrary.com]

TABLE 1 Chemical composition of steels used [w%]

	C	Si	Mn	P	S	N	Cu	Mo
S235J2 + N	0.107	0.176	1.02	0.014	0.001	-	0.016	0.002
S500G1 + M	0.056	0.208	1.58	0.012	0.002	0.004	0.273	0.175

	Ni	Cr	V	Nb	Ti	Al-T
S235J2 + N	0.020	0.023	0.001	-	-	0.041
S500G1 + M	0.516	0.056	0.001	0.02	0.001	0.033

"–"means <0.001.

The specimens of this study are welded with the flux cored arc welding process. Tack welds are used during welding to limit angular distortion and are later removed. The welding direction is normal to the rolling direction of the base material, and welding is performed with a 1.2-mm diameter Outershield 71E-H wire for S235 specimens and Stein Megafil 821R for S500 specimens. The welded plates are saw-cut from 1 m × 0.5 m plates into 500-mm-long, 50-mm-wide, and 10-mm-thick specimens that can be seen in Figure 2A. The clock-wise welding sequence of the details are presented in Figure 2B,C. Each weld was built by one weld layer.

The geometry of all specimens was measured prior to fatigue testing; this includes angular and axial misalignment, as well as the local weld geometry. Laser triangulation was used for the local weld geometry measurements, and the point data were analysed using the curvature method developed by Jung[35] (which was verified to yield consistent results by Schubnell et al[36]). The test specimen geometry and the local weld geometry parameter are schematically presented in Figure 2D,E. The measured throat thicknesses (a) averaged close to 5.5 and 6.4 mm for the S235 and S500 cruciform joints, respectively. For all cases, the flank angles (α) of the fillet welds were close to 135°, and the angular misalignment (φ) was below 1°; the axial misalignment (e) averaged around 7% of the plate thickness.

Fatigue testing is carried out under axial loading in the temperature chamber, with a temperature range of −180°C to +280°C on a Schenck horizontal resonance testing machine with maximum load capacity of 200 kN, at a frequency around 33 Hz and a nominal stress ratio of $R = 0$ (see Figure 3). Due to misalignment, however, the local stress ratio was slightly higher with $R < 0.15$. Failure is defined as full fracture of a specimen. Cooling is achieved using vaporized nitrogen from a liquid nitrogen tank, controlled by a chamber temperature gauge. During testing, the chamber and specimen temperatures are monitored by gauges; these are calibrated against an additional temperature gauge at RT that is positioned in the test lab and experiences only minor variations. As can be seen from Figure 3, the temperature is kept constant (within ±1°C). The spikes in max. and min. specimen temperatures are caused by nitrogen injection in the chamber.

3 | FATIGUE TEST RESULTS

All test results were statistically evaluated to obtain the mean stress-life (S-N) curve with

$$N = 2{\cdot}10^6 \left(\frac{\Delta\sigma_n}{\Delta\sigma_R}\right)^{-k} \quad (1)$$

where N is the endured number of cycles on the nominal stress range level $\Delta\sigma_n$, $\Delta\sigma_R$ is the reference fatigue strength at $2 \cdot 10^6$ cycles, and k is the slope of the S-N curve. The test results, evaluated based on a fixed slope exponent $k = 3$ (typical for welded joints[37]), are shown in

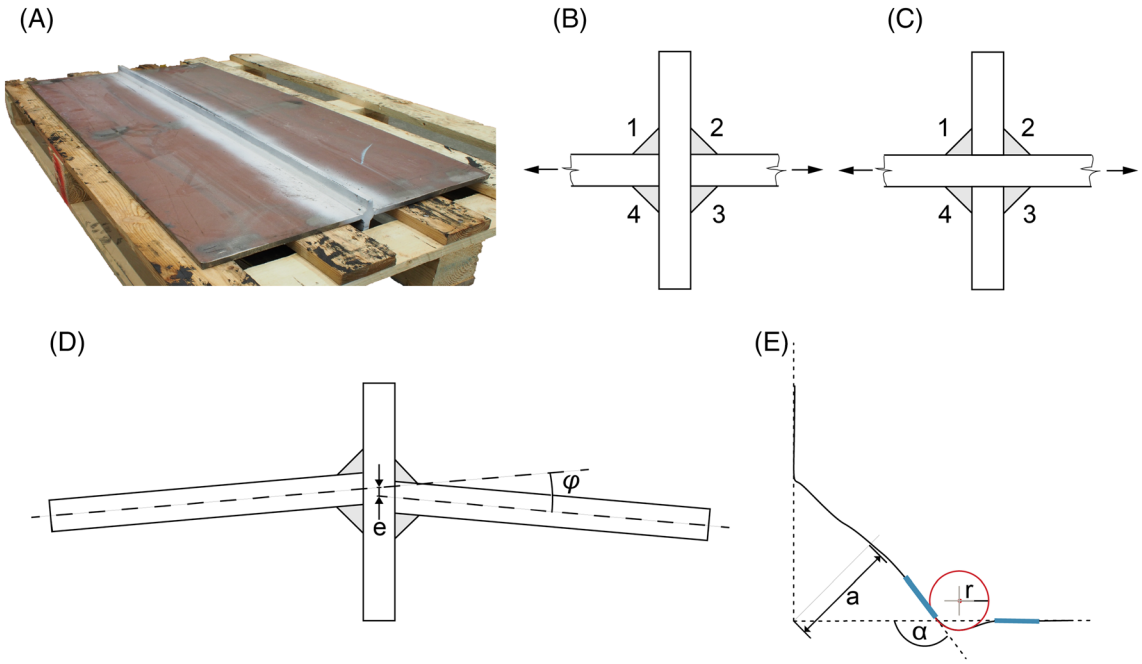

FIGURE 2 (A) Welded plate with welding sequence for (B) cruciform joint, (C) transversal stiffener, (D) misalignment description, and (E) local weld geometry [Colour figure can be viewed at wileyonlinelibrary.com]

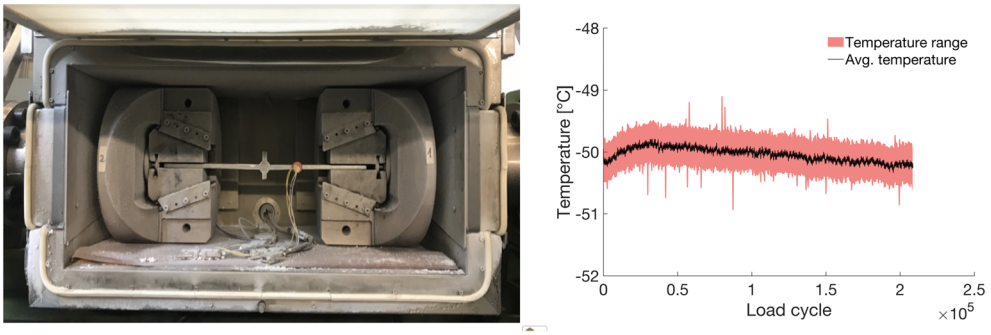

FIGURE 3 Temperature chamber for subzero temperature fatigue tests and temperature variation during fatigue test with mean temperature averaged over 30 s [Colour figure can be viewed at wileyonlinelibrary.com]

Figure 4. The mean and reference fatigue strength for probability of survival at $P_s = 50\%$ and 97.7% have been calculated and included in the figures alongside the scatter ratio (T_σ) between the fatigue strengths for $P_s = 90\%$ and 10%. All cruciform joint specimens showed root cracks resulting from the small weld size; all transverse stiffeners failed from the weld toes. Generally, all test series showed a clear improvement of fatigue strength as test temperature decreased. Moreover, the fatigue strength improvement seems to be comparable for all series; no decrease in fatigue strength is found for the normal-strength steels at -50°C. Even −30°C below the certified temperature of this steel grade, the fatigue strength seems to increase; this might be related to the high Charpy impact energy measured at the certified temperatures.

The analysis of the experimental data of the four test series shows that all test specimens, at all test temperatures, fulfil the requirements according to the corresponding FAT weld detail classes. It should be remarked that the fatigue strength for a probability of survival $P_s = 97.7\%$ at $N = 2 \cdot 10^6$ of the S235 transverse stiffener lies below the reference fatigue strength of FAT80 due to the relatively high scatter of this test series. As expected, the results confirm the general expectation that sharply notched as-welded steel joints made of high strength steel show comparable fatigue life to mild strength steel. Furthermore, the fatigue strength of the S500 cruciform joints is lower than the corresponding S235 weld detail; this might be related to the more convex fillet weld shape of the S500 cruciform joints, which can be seen from the macrographs. Interestingly, both weld details showed similar fatigue strength in terms of applied loading, but the larger cross-sectional area of the convex S500 fillet welds caused a reduced fatigue strength (in terms of nominal stress) compared with the S235 cruciform joints.

Due to the fact that the scatter ratio (T_σ) was generally very small, a clear trend towards higher fatigue strength at subzero temperatures can be seen from the S-N curves. The reason for the higher scatter of the S235 transverse stiffener S-N curves is caused by different numbers and locations of crack initiation sites. While the other three weld details always showed a large number of initiated cracks that grew together quickly, the S235 transverse stiffener sometimes had several cracks initiating in different planes (see Figure 5B); this can be intentionally caused with a weaving welding procedure but was not applied to the welded plates of this study. Moreover, specimens with almost no angular misalignment experienced simultaneous crack initiation at both the top and bottom side (see Figure 5B RT and −50°C).

Visual inspection of the fracture surfaces was performed to verify the fracture behaviour. As can be seen from Figure 5, large areas of the fracture surfaces of both cruciform joints and transverse stiffener specimens are dominated by fatigue crack propagation. At RT and −20°C, the fracture surfaces of the S235J2 + N transverse stiffener specimen show shear lips in the final rupture region; this indicates ductile failure. At −50°C, however, a cleavage crack perpendicular to the direction of the applied loading is visible; this is a clear sign for brittle material behaviour. In contrast, the S500G1 + M transverse stiffener specimen shows a fibrous fracture surface with some necking at both RT and −50°C, with shear lips at −20°C indicating ductile failure.

The fracture surfaces of the cruciform joints show similar behaviour. At RT, the fracture surfaces are characterized by a long crack propagation phase, and the final fracture is caused by plastic collapse (again, indicated by small shear lips). At −20°C, large areas of brittle fracture can be easily seen especially for the S500G1 + M cruciform joint in Figure 6. At −50°C, the shear lips are much smaller than at RT and −20°C (even for the S500 steel specimens), while they were still quite large for the transverse stiffener at −50°C. Both confirm that the DBTT temperature (and thus the FTT) is lower in the weld metal than in the base material. Although the cruciform joints failed by brittle fracture, the fatigue life was significantly longer at subzero temperatures compared with RT.

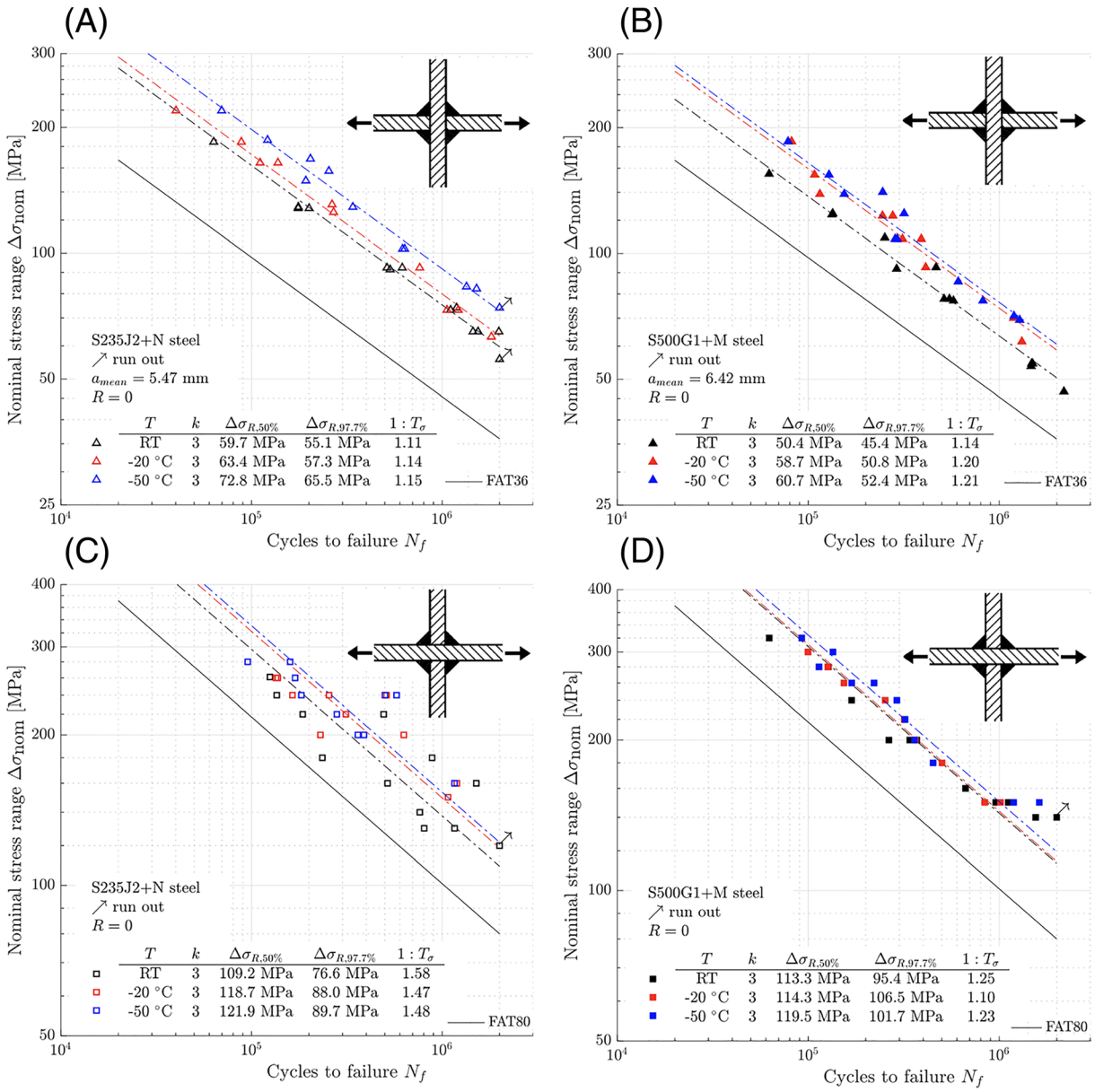

FIGURE 4 S-N diagram of (A) S235 J2 + N, (B) S500G1 + M cruciform joint, (C) S235 J2 + N, and (D) S500G1 + M transverse stiffener specimens with corresponding FAT36 and FAT80 weld detail classes [Colour figure can be viewed at wileyonlinelibrary.com]

4 | FURTHER TEST EVALUATION AND INFLUENCING FACTORS

From fatigue testing of full-scale and small-scale specimens, it is known that the residual stress level in small-scale fatigue test specimens is often lower than in full-scale structures. This fact has led to the conservative assumption of design codes that no residual stresses are present in small-scale specimens (see Hobbacher[37]). Consequently, fatigue test results of small-scale test specimens shall be corrected to a high stress ratio of $R = 0.5$, since fatigue design curves of welded joints are defined for that value,[37] in order to achieve comparable results for full-scale structures. When correcting results tested at a stress ratio of $R = 0$, a reduction of fatigue strength of 20% shall be applied according to IIW recommendations.[37] In recent years, this topic has gained new attention; alterations to the bonus-factor concept of the IIW recommendations for low residual stresses have been proposed, taking into account the mean-stress sensitivity dependent on joint type, residual stress level, and postweld treatment (see Hensel et al[38]). Despite huge progress in the field of residual stress measurements, in-depth measurements based on neutron diffraction—which is the preferred method for such applications—are still costly. Consequently, residual stresses at weld

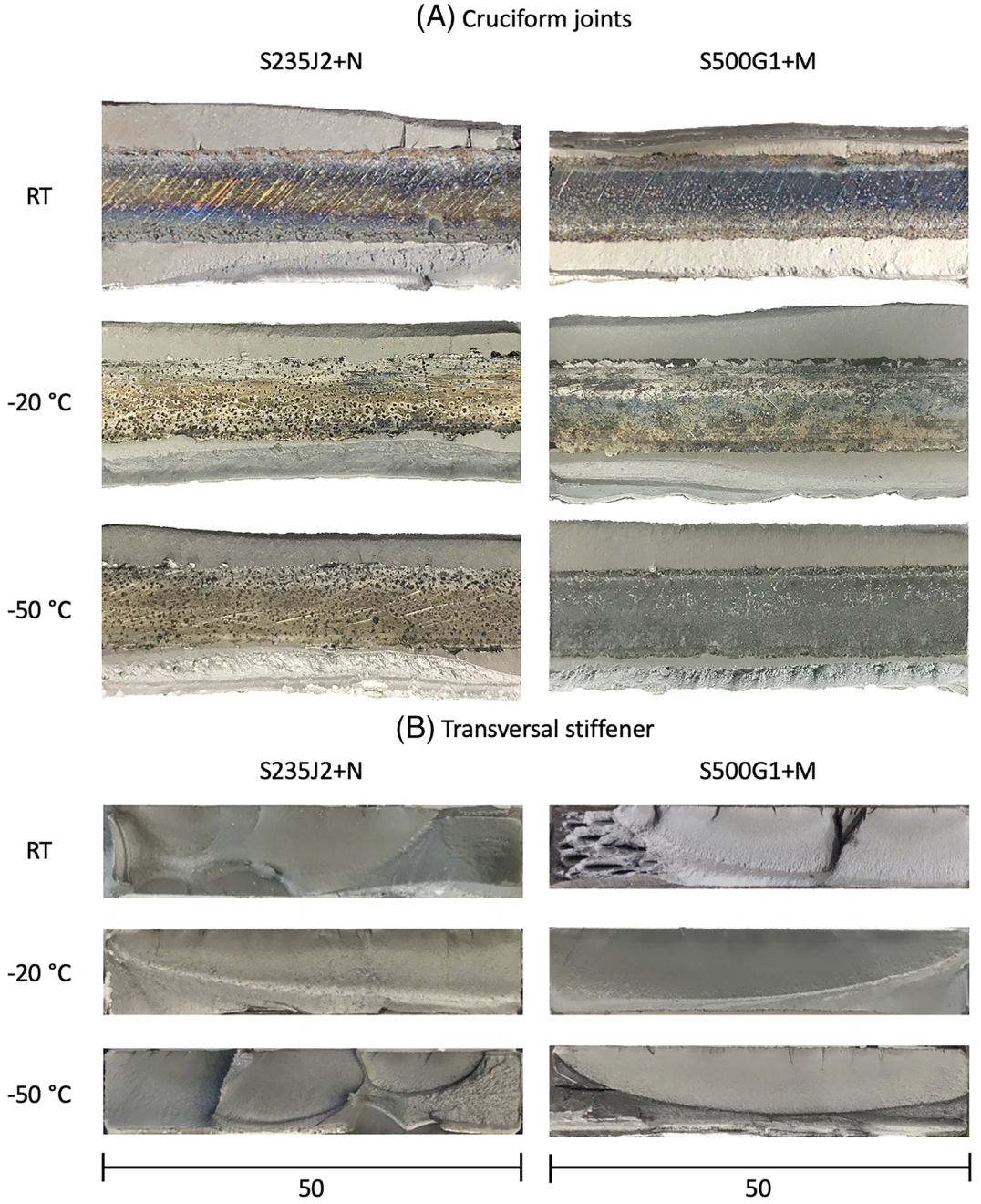

FIGURE 5 Fracture surface of (A) cruciform joint specimens (the figures show the fractured welds at top and bottom and the nonfused plate surface in the middle) and (B) transversal stiffener (scale in millimetres) [Colour figure can be viewed at wileyonlinelibrary.com]

roots in cruciform joints are difficult to measure. In order to investigate the mean stress sensitivity, additional tests at RT with a stress ratio of $R = 0.5$ were performed for three of the weld details. The results are presented as a comparison of the test series at $R = 0.5$ and $R = 0$ in Figure 6; these are summarized in Table 3.

Based on the results at $R = 0.5$ and $R = 0$, the mean stress sensitivity for the three compared cases can be calculated as the mean stress correction factor $f(R)$ by the ratio of mean fatigue strength ($\sigma_{R,mean}$) at $R = 0.5$ and $R = 0$ according to Equation (2).

$$f(R) = \frac{\Delta\sigma_{R,mean}(R = 0)}{\Delta\sigma_{R,mean}(R = 0.5)} \quad (2)$$

As can be seen from the summarized correction factors $f(R)$ in Table 3, the mean stress sensitivity is the same for the S500 cruciform joint and transverse stiffener, while it is smaller for the S235 cruciform joint weld detail. Moreover, the factors are smaller than the factor of $f(R) = 1.2$ recommended by IIW. The difference between the fatigue strength between $R = 0.5$ and $R = 0$ of the S235 cruciform joint is very small. Thus, the residual

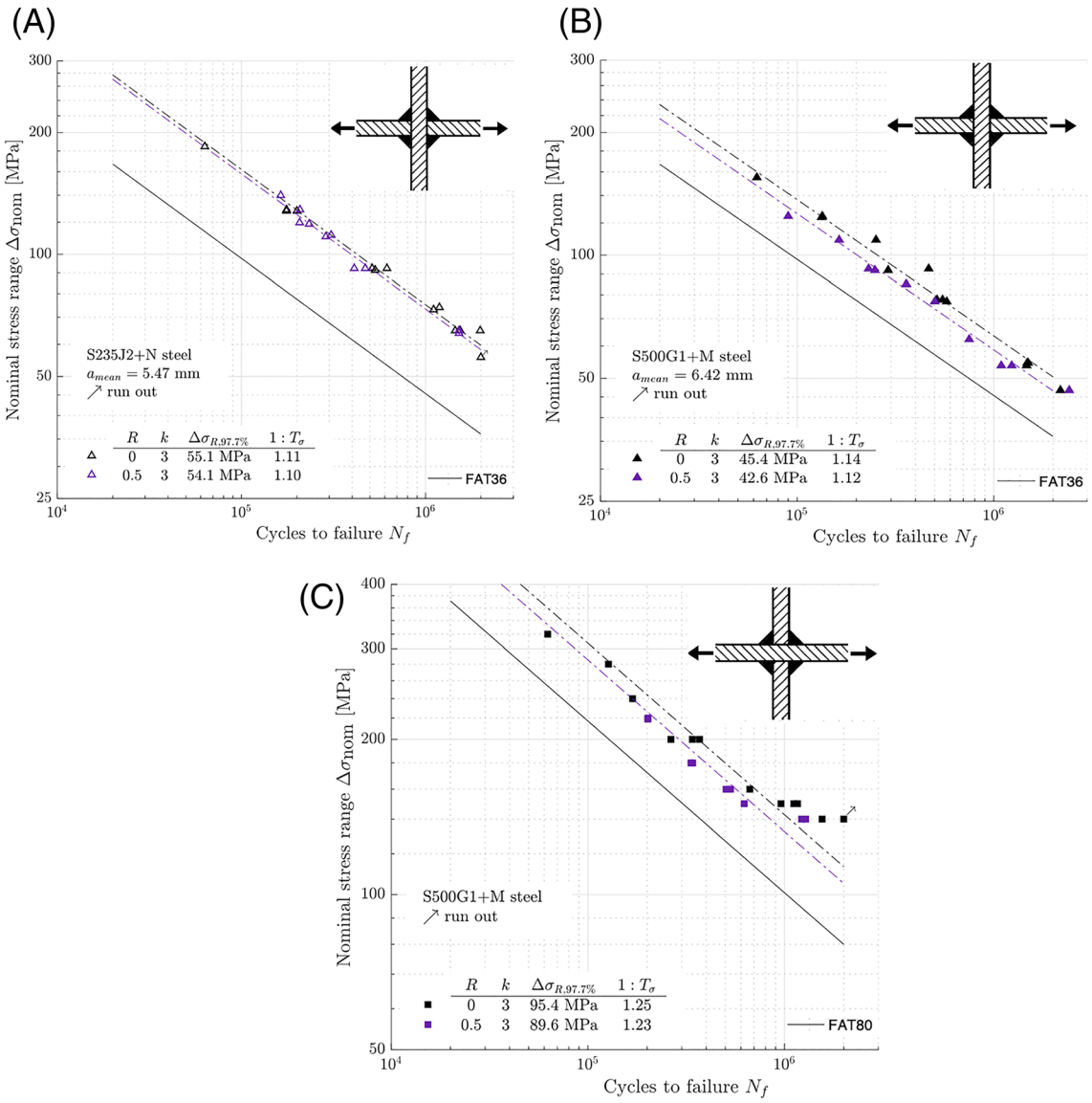

FIGURE 6 S-N diagram of (A) S235 J2 + N cruciform joint, (B) S235 J2 + N transverse stiffener specimens, and (C) S500G1 + M transverse stiffener specimens for stress ratios $R = 0$ and $R = 0.5$ [Colour figure can be viewed at wileyonlinelibrary.com]

stress level is probably close to the yield stress of the material in this case. A larger difference was found in the S500 test series. Consequently, the residual stress is smaller relative to the higher yield stress. The same mean stress correction factor was found for the S500 cruciform joint and transverse stiffener weld detail. Therefore, a similar level of residual stresses at weld toe and root can be expected. Since the same welding procedure was applied to the cruciform joint and transverse stiffener weld detail, it is assumed that the residual stress level at the weld toes of the S235 transverse stiffeners is also similar to the weld roots. Thus, the same correction factor as for the cruciform joints seems applicable.

To illustrate the increase of fatigue strength at subzero temperatures compared with RT, the results—in terms of the mean fatigue strength ($\Delta\sigma_{R,50\%}(T)$)—are normalized by the corresponding mean fatigue strength at 20°C $\Delta\sigma_{R,50\%}(T = 20\ ^\circ C)$. The fatigue strength ratio V_R is calculated according to Equation (3) and is shown in Figure 7A for the two different weld details and steel types.

$$V_R = \frac{\Delta\sigma_{R,50\%}(T)}{\Delta\sigma_{R,50\%}(T = 20°C)} \tag{3}$$

The assessed fatigue strength ratio increase is not constant for both weld details and steel types but shows a clear trend of higher fatigue strength at subzero temperatures. At −50°C, an almost identical increase for cruciform joints of both steels was measured, while the increase was different at −20°C. Moreover, a higher increase in fatigue strength was measured for the cruciform weld details than for transverse stiffener. The

TABLE 3 Fatigue test results with calculated mean and characteristic fatigue strength in [MPa] at $N = 2 \cdot 10^6$ evaluated using a fixed slope exponent $k = 3$

Test Series	Steel type	*R*-ratio	Mean fatigue strength	Characteristic fatigue strength	
Cruciform joints	S235J2 + N	0	59.7	55.1	1.03
	S235J2 + N	0.5	58.2	54.1	1.00
	S500G1 + M	0	50.4	45.4	1.08
	S500G1 + M	0.5	46.6	42.6	1.00
Transverse stiffener	S500G1 + M	0	113.3	95.4	1.08
	S500G1 + M	0.5	105.1	89.6	1.00

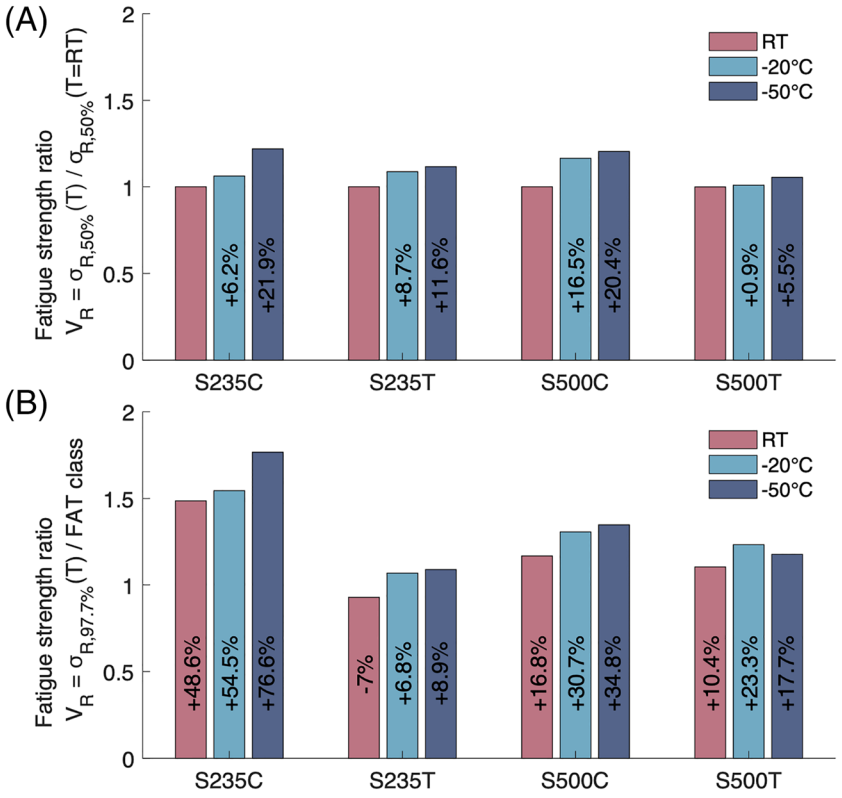

FIGURE 7 (A) Ratio of measured mean ($P_s = 50.0\%$, $N = 2 \cdot 10^6$) to mean fatigue strength at room temperature and (B) ratio of measured to corresponding fatigue strength class ($P_s = 97.7\%$, $N = 2 \cdot 10^6$) corrected to $R = 0.5$ with the mean stress correction factor $f(R)$ according to Table 3 [Colour figure can be viewed at wileyonlinelibrary.com]

smallest increase of fatigue strength was found for the S500 transverse stiffener weld detail. It is important to note that more testing is required to completely rule out statistical uncertainty.

$$V_R = \frac{\Delta\sigma_{R,97.7\%,R=0.5}(T)}{\Delta\sigma_{R,FAT}} \tag{4}$$

To illustrate the difference between fatigue strength at subzero temperatures and the IIW design recommendations,[37] the results in terms of the fatigue strength $\Delta\sigma_{R,97.7\%}$ at $N = 2 \cdot 10^6$ cycles for a probability of survival of $P_s = 97.7\%$ are normalized by the corresponding IIW design fatigue strength $\Delta\sigma_{R,FAT}$. The so calculated fatigue strength ratio V_R according to Equation (4) is shown in Figure 7B corrected to $R = 0.5$ with the mean stress correction factor $f(R)$ according to Table 3.

5 | REVIEW OF TEMPERATURE EFFECT ON DESIGN CURVES

As initially mentioned, data on fatigue strength of welded steel joints at subzero temperatures are scarce; however, more data are available for notched and unnotched base material specimens. To the authors' best knowledge, the oldest studies date back to the 1930s, with the first extensive data collection by Hempel and Luce.[39] Probably, the most comprehensive collection of the temperature effect on fatigue strength dates back to the 1960s and 1980s. Forrest[40] and Stephens et al[25] collected data from

literature for different materials like steel, aluminium, and titanium alloys with temperatures ranging from RT to cryogenic temperatures. Unsurprisingly, the fatigue strength increase was several magnitudes larger in the unnotched case. Schijve[41] and Radaj and Vormwald[42] related this fact to the higher notch sensitivity at low temperatures caused by the increase in yield strength at low temperatures; this, in turn, is related to the increased resistance against plastic deformation caused by the lower mobility of dislocations. Another way of describing the change of fatigue properties is by relating the fatigue strength to the change of Young's modulus with temperature. Wang et al[43] and Outinen and Mäkeläinen[44] measured Young's modulus at temperatures between 20°C and 950°C for higher-strength and high-strength steel, showing a decrease of roughly 10 GPa for every 100°C increase up to 500°C. Based on these studies and other published data,[45] a linear trend extending into the subzero temperature domain might be expected. Data on stress-strain behaviour of structural steel are rare and usually exhibit a scattered pattern; this might be an artefact of the sensing technology. Paik et al,[46] for example, measured higher mean Young's modulus values at −20°C than at RT and −60°C for AH32 and DH32 steel grades, while Ehlers and Østby[47] reported no change at all. The IIW recommendations[37] also correlate fatigue strength at high temperature to the change of Young's modulus at high temperatures E_{HT}.

$$FAT_{HT} = FAT_{20°C}\frac{E_{HT}}{E_{20°C}} \tag{5}$$

This formula seems to be based on BS 7910,[48] where Equation (50) relates the threshold stress intensity factor K_0 of nonferrous metals to the threshold stress intensity factor of steels via the Young's modulus of steel, see Equation (6).

$$K_0 = K_{0,steel}\frac{E}{E_{\text{steel}}} \tag{6}$$

Here, no comment is given regarding the applicability of this formula for changing Young's modulus with temperature. However, since the same formula for the changing intersection point A of the simplified FCG curve is used for the calibration for nonferrous metals (Equation 7) and high temperatures (Equation 8), it can be assumed that Equation (6) is valid for changing Young's modulus at high temperatures E_{HT} as well.

$$A = 5.21{\cdot}10^{-13}\left(\frac{E_{\text{steel}}}{E}\right)^3 \tag{7}$$

$$A = 5.21{\cdot}10^{-13}\left(\frac{E_{RT}}{E_{HT}}\right)^3 \tag{8}$$

Moreover, BS 7910[48] includes a table based on American Society of Mechanical Engineers (ASME) Boiler and Pressure Vessel Code (BPVC) Section 2 Materials Part D: Properties,[45] which states the change of Young's modulus for ferritic and austenitic steel at temperatures between −200°C and 650°C. For temperatures above 200°C, a similar change is given as in Wang et al[43] and Outinen and Mäkeläinen,[44] while the change from 25°C to −50°C is comparably low with 4 GPa.

Based on a Young's modulus of approximately 205 GPa at 25°C, considered here as comparable to RT, an increase of about 1% in fatigue strength would be expected for a temperature of −20°C and 2% for −50°C. The increase found in this study was, however, much higher, leading to the conclusion that the Young's modulus might increase more at subzero temperatures than expected by ASME BPVC.[45] Moreover, measurements of Young's modulus are already highly scattered at RT, making it difficult to accurately measure it at low temperatures. Since the formula given by the IIW recommendations[37] is actually meant for high temperatures and not validated for low temperatures, it does not seem applicable to subzero temperatures.

The German FKM guideline is another standard that include a correction factor based on service temperature.[49] Although the guideline states that low temperatures are outside its scope and that no correction shall be applied in the range of −40°C to 60°C, the given empirical formula for temperatures above 100°C might, due to its formulation, yield reasonable results for subzero temperatures as well. As in the IIW recommendations,[37] a linear relation between fatigue strength and temperature is assumed according to Equation (9), with the correction factor $K_{T,D}$ from Equation (10):

$$\sigma_{w,T} = K_{T,D}\sigma_{w,T=20°C} \tag{9}$$

$$K_{T,D} = 1 - 1.4{\cdot}10^{-3}{\cdot}(T - 100);\ T \text{ in } [°\text{C}] \text{ for } T > 100°C. \tag{10}$$

Setting the reference to 20°C, an increase of fatigue strength of 5.6% would be expected compared with RT and 9.8% from RT to −50°C. Compared with the IIW recommendations,[37] a much higher increase is calculated at subzero temperatures. Moreover, the measured increase in fatigue strength based on Equation (9) would be conservative for all test series except the S500 transverse stiffener.

6 | DISCUSSION

The study has shown that there is a clear fatigue strength dependence on low temperatures for welded joints, which confirms the results of earlier studies on FCG rate testing of base materials (eg, Walters et al,[29] Alvaro et al[31]) as well as on fatigue strength of longitudinal stiffeners at subzero temperatures (see Bridges et al[3]). The increase in fatigue strength of the tested weld details was found to be in the same order of magnitude for both steels. Most importantly, no decrease of fatigue strength was found for the normal strength steel with a nominal lowest design temperature of −20°C, even at a test temperature of −50°C. Consequently, welded joints with weld toe and weld root failure made of a normal strength steel are assumed to be safe even at the lowest design temperatures defined by Hauge et al,[13] being −40°C. Thereby, the findings of Walters et al[16] regarding fracture toughness requirement over fulfilment at subzero temperatures are supported for fatigue strength of welded joints. Interestingly, a larger increase in fatigue strength was found for cruciform joints with root failure compared with transverse stiffener with weld toe failure. Although transverse stiffener specimens show a longer crack initiation period for which higher temperature effect would be expected, the increase in fatigue strength for this weld detail was smaller than for the cruciform joint detail. From FCG rate measurements by Walters et al[29] and Alvaro et al,[31] a stronger decrease in FCG rate was found in the low stress-intensity factor range than in the intermediate and higher region of the Paris-curve. Further investigation is required to explain the smaller increase observed for the transverse stiffener's fatigue strength. Although, the mean fatigue strength of the transverse stiffener at RT is almost the same as the S235 transverse stiffener specimens, the latter experienced a higher fatigue strength increase at subzero temperatures. While fatigue cracks initiate in the weld metal in case of the cruciform joint weld detail, they initiate in the HAZ for the transverse stiffener.

From literature, it is known that the fracture toughness—and thereby the DBTT and FDBT—are often least favourable in the HAZ and at the fusion line.[34] In their FCG tests of S460 structural steel, Walters et al[29] found a FTT which was approximately 18°C higher than the T_{27J} DBTT from Charpy notch impact testing. More recently, Alvaro et al[32] found a difference of 15°C between the FTT and DBTT in weld simulated 420 MPa steel. It might therefore be possible that temperatures below the FTT of the HAZ cause the increases in fatigue strength to be smaller for transverse stiffeners than for cruciform joints. Walters et al[29] and Alvaro et al,[31,32] however, measured only a slight increase of the threshold stress intensity factor range below the FTT; this would explain why the fatigue strength at −50°C is still above the fatigue strength at −20°C. Although, S-N tests are not well suited to measure the FTT due to the large number of specimens needed for each curve, the constant increase in fatigue strength at subzero temperatures verifies that the fatigue strength of welded joints seems to stay above the fatigue strength at RT for temperatures corresponding to Arctic conditions.

In summary, a high fatigue strength increase at 50°C was found for the cruciform joint weld detail, with an increase of about 20% when comparing the S235 J2 + N normal strength and the S500G1 + M high-strength steel with RT. The transverse stiffener weld detail, in contrast, showed an increase of about 12% for the S235J2 + N and 6% for the S500G1 + M steel at this temperature. Comparing this increase to the empirical formulas by the German FKM guideline,[49] the increase would be correctly estimated for the S500G1 + M transverse stiffener, while being conservative in all other cases. Assuming a change of Young's modulus of 4 GPa from RT to −50°C (based on BS7910[48] and ASME BPVC[45]) and applying the formula given by the IIW design recommendations[37] leads to overly conservative results; however, those formulas are only meant for high temperature fatigue. Applicability to subzero temperatures was investigated in this study since no correction formulas for subzero temperatures currently exist. Additionally, Young's modulus is a varying quantity due to factors such as rolling of plate material, thickness effects, sensing technology, etc. Thus, it might not be particularly suitable to describe the temperature effect on fatigue strength.

7 | CONCLUSIONS

This study investigated the fatigue strength of fillet welded joints of a normal and a high strength steel at room and at subzero temperatures by means of S-N tests; experimental results were compared with estimates based on international standards. The following conclusions can be drawn from the investigation:

- Compared with RT, the fatigue strength of fillet welded joints of normal and high strength steel seems to increase constantly with decreasing temperature throughout the tested range. The average fatigue strength increases by 8% at −20°C and 15% at −50°C.
- The highest increases in fatigue strength, of approximately 22%, have been found at −50°C for a normal-strength steel grade that is only qualified for −20°C (based on fracture toughness properties). This extends the findings of Walters et al[16] that steel grades for

higher temperatures often fulfil fracture toughness requirements at much lower temperatures to fatigue strength at subzero temperatures.

- Although visual inspections of the fracture surfaces reveal brittle fracture areas, the fatigue strength increases more at lower temperatures.
- Comparison with design curves and correction factors show overconservatism of some standards, whose applicability is already doubtful. Calculating the fatigue strength increase based on estimates of Young's modulus according to IIW recommendations,[37] BS7910,[48] and ASME BPVC[45] leads to more conservative results than the empirical formulae in the FKM guideline.[49]
- The Young's modulus of a material varies due to several different factors and thus might not be suitable to describe the temperature effect on fatigue strength.
- Finally, fatigue design curves for welded joints derived from tests at RT can be safely applied to temperatures as low as −50°C, but highly underestimate the actual fatigue strength at subzero temperatures; this is especially true for cruciform joints.

NOMENCLATURE

A	= Constant in fatigue crack growth relation
a	= Weld throat thickness
CVN	= Charpy V-notch impact toughness
E_{HT}	= Young's modulus at high temperatures
E_{RT}	= Young's modulus at room temperatures
E_{steel}	= Young's modulus of steel
$E_{20\,^\circ C}$	= Young's modulus at a temperature of 20°C
FAT_{HT}	= Fatigue strength for high temperatures at $2 \cdot 10^6$ cycles for a probability of survival 95% and a confidence level of 75%
$FAT_{20\,^\circ C}$	= Fatigue strength at $2 \cdot 10^6$ cycles for a probability of survival 95% and a confidence level of 75% at 20 °C
e	= Axial misalignment
e_f	= Elongation at fracture
$f(R)$	= Mean stress correction factor
k	= Slope exponent of the stress-life curve
$K_{T,D}$	= Fatigue strength correction factor acc. to the FKM guideline
N	= Number of cycles to failure
P_s	= Probability of survival
r	= Weld toe radius
R	= Stress ratio between lower and upper stress
T	= Temperature
T_σ	= Scatter ratio $(1/(\Delta\sigma_{R,10\%}/\Delta\sigma_{R,90\%}))$
V_R	= Fatigue strength ratio
α	= Weld flank angle
K_0	= Threshold stress intensity factor of non-ferrous metals
$K_{0,steel}$	= Threshold stress intensity factor of steel
$\Delta\sigma_n$	= Nominal stress range
$\Delta\sigma_{R,FAT}$	= Reference fatigue strength at $2 \cdot 10^6$ corresponding to the IIW FAT class
$\Delta\sigma_{R,i}$	= Reference fatigue strength at $2 \cdot 10^6$ cycles for a probability of survival i
$\Delta\sigma_{R,i,\ R\,=\,0.5}$	= Reference fatigue strength at $2 \cdot 10^6$ cycles for a probability of survival i and a stress ratio $R = 0.5$
$\Delta\sigma_{R,mean}$	= Mean fatigue strength at $2 \cdot 10^6$ cycles for a probability of survival of 50%
$\sigma_{w,T}$	= Fatigue strength acc. to the FKM guideline at a temperature T
$\sigma_{w,T\,=\,20\,^\circ C}$	= Fatigue strength acc. to the FKM guideline at a temperature of 20°C
σ_{UTS}	= Ultimate tensile strength
σ_{YS}	= Yield strength
φ	= Angular misalignment

ACKNOWLEDGEMENTS

The work was performed within the research project ESM-50 "Fatigue of welded structures at subzero temperatures," funded by the German Research Association of the Working Group of the Iron- and Metal-processing Industry e.V. as part of the Donors' Association for the Promotion of Sciences and Humanities in Germany under project number AVIF-No. A 301.

ORCID

Moritz Braun https://orcid.org/0000-0001-9266-1698

REFERENCES

1. von Bock und Polach RU, Klein M, Kubiczek J, Kellner L, Braun M, Herrnring H. State of the art and knowledge gaps on modelling structures in cold regions. ASME 2019 38th International Conference on Offshore Mechanics and Arctic Engineering—OMAE 2019; 2019; Glasgow, Scotland.
2. Baek J-H, Kim C-M, Kim W-S, Kho Y-T. Fatigue crack growth and fracture toughness properties of 304 stainless steel pipe for LNG transmission. *Metals and Materials International*. 2001;7(6):579-585.
3. Bridges R, Zhang S, Shaposhnikov V. Experimental investigation on the effect of low temperatures on the fatigue strength

of welded steel joints. *Ships and Offshore Struct*. 2012;7(3):311-319.

4. Jeong D, Lee S, Seo I, Yoo J, Kim S. Fatigue crack propagation behavior of Fe24Mn steel weld at 298 and 110 K. *Metals and Materials International*. 2015;21(1):22-30.
5. Jung D-H, Kwon J-K, Woo N-S, Kim Y-J, Goto M, Kim S. S–N Fatigue and fatigue crack propagation behaviors of X80 steel at room and low temperatures. *Metal Mater Trans A*. 2013;45(2):654-662.
6. Kang K-W, Goo B-C, Kim J-H, Kim D-K, Kim J-K. Experimental investigation on static and fatigue behavior of welded sm490a steel under low temperature. *Int J Steel Struct*. 2009;9(1):85-91.
7. Kim S, Jeong D, Sung H. Reviews on factors affecting fatigue behavior of high-Mn steels. *Metals and Materials International*. 2018;24(1):1-14.
8. Li ZR, Zhang DC, Wu HY, Huang FH, Hong W, Zang XS. Fatigue properties of welded Q420 high strength steel at room and low temperatures. *Construct Build Mater*. 2018;189:955-966.
9. Liao XW, Wang YQ, Qian XD, Shi YJ. Fatigue crack propagation for Q345qD bridge steel and its butt welds at low temperatures. *Fatigue Fract Eng Mater Struct*. 2018;41(3):675-687.
10. Shulginov B, Matveyev V. Impact fatigue of low-alloy steels and their welded joints at low temperature. *In J Fatig*. 1997;19(8-9):621-627.
11. Lloyd's Register Group Limited. *ShipRight design and construction fatigue design assessment FDA ICE fatigue induced by ice loading*. London, UK: Lloyd's Register Group Limited. 2011.
12. ISO. *19906:2010(E): Petroleum and natural gas industries—Arctic offshore structures*. Geneva, Switzerland: ISO; 2010.
13. Hauge M, Maier M, Walters CL, et al. Status update of ISO TC67/SC8/WG5: materials for arctic applications. The 25th International Ocean and Polar Engineering Conference; 2015; Kona, Hawaii, USA.
14. ISO. *19902:2007: Petroleum and natural gas industries—fixed steel offshore structures*. Geneva, Switzerland: ISO; 2007.
15. Maddox SJ. Fatigue Strength of Welded Structures. 2nd ed: Woodhead Publishing; 2002.
16. Walters CL, Dragt RC, Romeijn E, van der Weijde G. Use of current S355 and S690 steels for arctic applications. The 24th International Ocean and Polar Engineering Conference; 2014; Busan, Korea.
17. McClintock RM, Gibbons HP. Mechanical properties of structural materials at low temperatures. National Bureau of Standards; 1960.
18. Alvaro A, Akselsen OM, Ren XB, Kane A. Fundamental aspects of fatigue of steel in Arctic applications. The 24th International Ocean and Polar Engineering Conference; 2014; Busan, Korea.
19. Suyuthi A, Leira BJ, Riska K. Fatigue damage of ship hulls due to local ice-induced stresses. *App Ocean Res*. 2013;42:87-104.
20. Hamdoon M, Das S, Zamani N. Effect of combined cold temperature and fatigue load on performance of G40.21 Steel. *Materials Performance and Charact*. 2014;3(1): 49-64, 20130030.
21. El-Shabasy AB, Lewandowski JJ. Effects of load ratio, R, and test temperature on fatigue crack growth of fully pearlitic eutectoid steel (fatigue crack growth of pearlitic steel). *In J Fatig*. 2004;26(3):305-309.
22. Kawasaki T, Yokobori T, Sawaki Y, Nakanishi S, Izumi H. Fatigue fracture toughness and fatigue crack propagation in 5.5% Ni steel at low temperature. International Conference on Fracture (ICF4); 1977; Waterloo, Canada.
23. Lü B, Zheng X. Predicting fatigue crack growth rates and thresholds at low temperatures. *Mater Sci Eng A*. 1991;148(2):179-188.
24. Moody NR, Gerberich WW. Fatigue crack propagation in iron and two iron binary alloys at low temperatures. *Mater Sci Eng A*. 1979;41(2):271-280.
25. Stephens RI, Chung JH, Glinka G. Low temperature fatigue behavior of steels—a review. *SAE Transactions*. 1979;88(2): 1892-1904.
26. Stonesifer FR. Effect of grain size and temperature on fatigue crack propagation in A533 B steel. *Eng Fract Mech*. 1978;10(2): 305-314.
27. Vogt J-B, Magnin T, Foct J. Effective stresses and microstructure in cyclically deformed 316 l austenitic stainless steel: effect of temperature and nitrogen content. *Fatigue Fract Eng Mater Struct*. 1993;16(5):555-564.
28. Walters CL. The effect of low temperatures on the fatigue of high-strength structural grade steels. 20th European Conference on Fracture; 2014.
29. Walters CL, Alvaro A, Maljaars J. The effect of low temperatures on the fatigue crack growth of S460 structural steel. *In J Fatig*. 2016;82:110-118.
30. Wallin K. Fracture toughness transition curve shape for ferritic structural steels. In: Teoh SH, Lee KH, eds. *Fracture of Engineering Materials and Structures*. Springer: Dordrecht; 1991:83-88.
31. Alvaro A, Akselsen OM, Ren XB, Nyhus B. Fatigue crack growth of a 420 MPa structural steel heat affected zone at low temperatures. The 26th International Ocean and Polar Engineering Conference; 2016; Rhodes, Greece.
32. Alvaro A, Akselsen OM, Ren XB, Perillo G, Nyhus B. On the relation between fatigue and static ductile to brittle transition for weld simulated 420 MPa structural steel. Paper presented at: The 27th International Ocean and Polar Engineering Conference2017; San Francisco, USA.
33. Fang X-Y, Cai Z-B, Wang J-G, Yang X-F. Evaluation of temperature-sensitive fatigue crack propagation of a high-speed railway wheel rim material. *Fatigue Fract Eng Mater Struct*. 2019;42(8):1815-1825.
34. Anderson T, McHenry H. *Fracture toughness of steel weldments for arctic structures*. Boulder, Colorado: National Bureau of Standards; 1982.
35. Jung M. Development and implementing an algorithm for approximation and evaluation of stress concentration factors of fillet welds based on contactless 3D measurement [master thesis], Karlsruher Institut für Technologie; 2018.
36. Schubnell J, Jung M, Le CH, et al. Influence of the optical measurement technique and evaluation approach on the determination of local weld geometry parameters for different weld types. Welding in the World. 2019; submitted for publication.
37. Hobbacher A. *Recommendations for fatigue design of welded joints and components*. 2nd ed: Springer International Publishing Switzerland: Springer; 2016.

38. Hensel J, Nitschke-Pagel T, Dilger K. Engineering model for the quantitative consideration of residual stresses in fatigue design of welded components. *Welding in the World*. 2017;61(5):997-1002.
39. Hempel M, Luce J. Verhalten von Stahl bei tiefen Temperaturen unter Zug-Druck-Wechselbeanspruchung. *Archiv für das Eisenhüttenwesen*. 1942;15(9):423-430.
40. Forrest PG. *Fatigue of Metals*. 14 Oxford: Pergamon Press Ltd.; 1963.
41. Schijve J. *Fatigue of Structures and Materials*. Netherlands: Springer; 2009.
42. Radaj D, Vormwald M. *Ermüdungsfestigkeit: Grundlagen für Ingenieure*. 3rd ed: Springer Berlin Heidelberg; 2007.
43. Wang WY, Liu B, Kodur V. Effect of Temperature on strength and elastic modulus of high-strength steel. *J Mater Civil Eng*. 2013;25(2):174-182.
44. Outinen J, Makelainen P. Mechanical properties of structural steel at elevated temperatures and after cooling down. *Fire Mater*. 2004;28(2-4):237-251.
45. American Society of Mechanical Engineers. *ASME Boiler & Pressure Vessel Code—Section 2: Materials—Part D: Properties*. New York: American Society of Mechanical Engineers, 2017.
46. Paik JK, Kim KJ, Lee JH, Jung BG, Kim SJ. Test database of the mechanical properties of mild, high-tensile and stainless steel and aluminium alloy associated with cold temperatures and strain rates. *Ships and Offshore Struct*. 2017;12(sup1):S230-S256.
47. Ehlers S, Østby E. Increased crashworthiness due to arctic conditions—the influence of sub-zero temperature. *Marine Structures*. 2012;28(1):86-100.
48. BS 7910:2013 + A1:2015 Guide to methods for assessing the acceptability of flaws in metallic structures. The British Standards Institution; 2015.
49. FKM-Richtlinie. Rechnerischer Festigkeitsnachweis für Maschinenbauteile aus Stahl, Eisenguss- und Aluminiumwerkstoffen. 6. ed. Frankfurt/Main: VDMA-Verlag; 2012.

How to cite this article: Braun M, Scheffer R, Fricke W, Ehlers S. Fatigue strength of fillet-welded joints at subzero temperatures. *Fatigue Fract Eng Mater Struct*. 2020;43:403–416. https://doi.org/10.ffe.13163